

Accurate Area and Width Measurements from Neutron Beam Computed Tomography (NBCT) Images of Cooling Holes of a Used Tornado Jet Engine Turbine Blade by a CAD Based on the De-Convolution Technique

Kui-Ming CHUI¹, Shu-Yan ZHANG², Eberhard LEHMANN³, Anders KAESTNER³, Shyr-Lin CHUI⁴,
Andrew WRIDE¹, David STANFIELD¹

¹Image Enhancement Technology Ltd, 8 Gilbey Close, Ickenham, Uxbridge, Middlesex, UK, UB10 8TD.
Phone: +44 1895 635203; e-mails: ming-chui@iet.org.uk, andrew.wride@lineone.net, dbs@iet.org.uk

²Science and Technology Facilities Council, Rutherford Appleton Laboratory, Didcot, Oxfordshire, OX11 0QX,
UK. e-mail: shu-yan.zhang@stfc.ac.uk

³Spallation Neutron Source Division, Paul Scherrer Institut, ASQ Division WB BA/112, 5232 Villigen PSA.,
Switzerland. E-mails: eberhard.lehmann@psi.ch, anders.kaestner@psi.ch

⁴University Hospital of Northern British Columbia, BC, Canada. e-mail: shyrchui@netscape.net

Abstract

Blurred image edges caused by the Penumbra Effect have existed since the discovery of X-rays. In Computed Tomography (X-ray or Neutron-Beam), the combined effect of the sizes of the energy source and the detector(s) cause the Penumbra Spread. Recently, by using the processing power of modern CPUs, we have found a software solution to the problem - a post-processing De-Convolution Technique for the detection, definition, and enhancement of image edge profiles. Enhancement is carried out in a zoomed space within which the higher the magnification factor, the clearer the enhanced image, as both the Penumbra and the Pixelization Effects are overcome simultaneously. The overall effect is to re-focus the image edge-profile, as if derived from an infinitely small energy source. This patented technique has all the advantages of sensitivity, sub-pixel accuracy, and efficiency (in terms of processing-time). By solving this previously 'unsolvable' problem, numerous important applications may now be realized.

Keywords: Neutron Beam Computed Tomography, image enhancement, De-Convolution Technique, NDT, accurate measurement.

1. Introduction

1.1 Object or Purpose of Study

The Penumbra Effect describes blurring at the margins of an image profile due to the finite size of the energy source. A computer aided detection (CAD) algorithm based on the De-Convolution Technique can be used to pinpoint true edge positions to sub-pixel accuracy and remove the Penumbra Effect (and at the same time, the removal of the Pixelization Effect) via sub-pixel transfers without trade-off losses [1]. Derived from this, a definitive method of accurate measurement may have been found. 50 slices of NBCT images on four cooling holes of a used jet turbine blade were analysed to study the merits of the algorithm on both the detection of minute defects such as fractures and distortion and the accurate measurement of the cross-sectional areas of the cooling holes.

2. Specific Experimental Details

2.1 Materials, Methods, and Procedures

2.1.1. Composite phantom and New-York Catphan-500 were used to provide X-ray CT images to verify the accuracies of the De-Convolution Technique [1 & Section 2.2].

2.1.2. The Technique of Neutron-Beam Computed Tomography (NBCT)

The neutron-beam imaging experiment was performed at the cold neutron imaging beamline ICON of the SINQ spallation neutron source at the Paul Scherrer Institut (PSI) [2]. The neutrons at the beamline originate from the

cold moderator of the SINQ (25K) and have an energy spectrum with peak at 25meV and an average energy of 8.5meV. Using the high-resolution imaging setup at experiment position 2 and a neutron aperture of 20mm the collimation ratio was $L/D=340$. This was sufficient to assume parallel beam geometry for the given sample size. The pixel size was 13.5 microns and the resolution 21 lp/mm. The CT projection data consisted of 625 projections (2048x2048 pixels) on a 360 degrees scan. The projection data was reconstructed using a filtered back-projection algorithm for parallel beam.

2.2 Results

2.2.1 Phantom Calibration by X-ray CT

Measurements: Distance – at high-contrast and 1% low-contrast edge, both accurate to $1/50^{\text{th}}$ of a pixel. Area/Volume - at high-contrast and 1% low-contrast edge, accurate to $1/18^{\text{th}}$ and $1/10^{\text{th}}$ of a pixel respectively. Modulation Transfer Function (MTF) [3] – improved from 3.38 lp/cm to 9.61 lp/cm at 50% modulation level after 7x magnification and enhancement. Processing time - 7x magnification and enhancement of region of interest (ROI) of size 107×107 pixel² (or 749×749 sub-pixel²) took 1.17 seconds using a 2.4GHz-CPU.

2.2.2 NBCT images – 505 Neutron-Beam CT image slices through a jet turbine blade, end to end, (0.013mm/slice) were collected.

2.2.3 Field Examples

A used Tornado jet engine turbine blade (C3FOX) was analysed. To cover the complete blade, 505 slices of thickness 0.0135mm/slice were obtained. 50 slices starting from #0520, #0530, (step 10), ... to #1010 were analysed. An additional noise filter was added in to help with the analysis. Figure 1 shows the original image of Slice #0520 with ROI placed on the four cooling holes of A(12 o'clock), B(9 o'clock), C(6:30 o'clock) and D(3 o'clock). Figure 2 - the 7x magnification of the ROI 'before' enhancement, Figure 3 - the 7xROI 'after' enhancement, and Figure 4 - the enhanced image with its edge-dot profiles included for the detection of defects as well as for the contour-outlining the area.

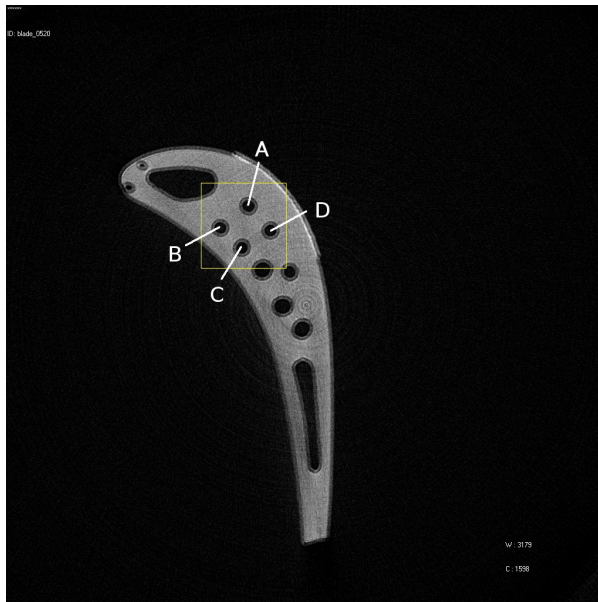


Figure 1: Original image with ROI on 4 cooling holes

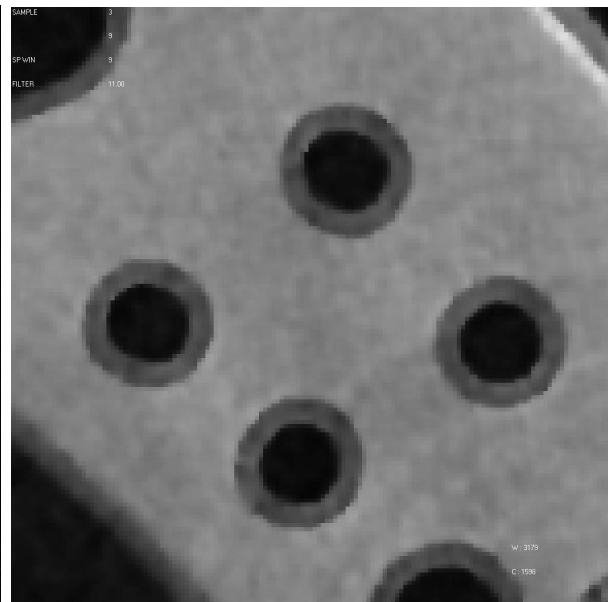


Figure 2: 7x ROI 'before' enhancement

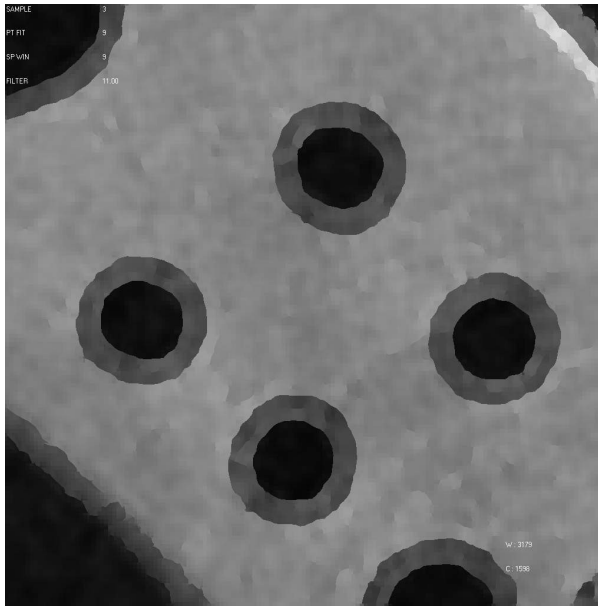


Figure 3: 7x ROI 'after' enhancement ...

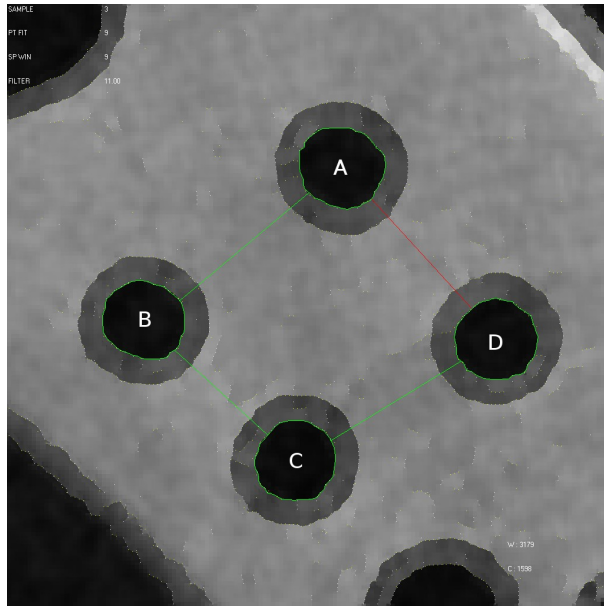


Figure 4: ... with edge-dot profiles and annotations

2.2.1.1 Cross-Sectional Area

The cross-sectional area of the four cooling holes, A, B, C & D versus the slice positions were measured and plotted in Figure 5.

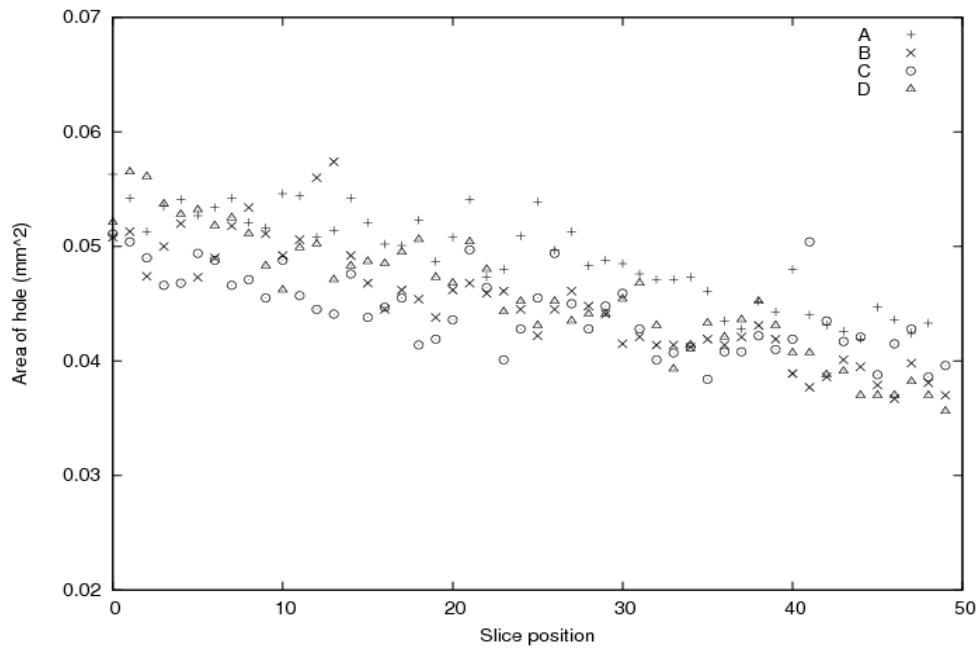


Figure 5: Area of cooling hole versus slice-position

The areas of the four holes varied across the slice set (Table 1).

Table 1. Areas of Holes

| Hole | Max. (mm²) | Min. (mm²) | Diff. (%) |
|-------------|------------------------------|------------------------------|------------------|
| A | 0.0563 | 0.0419 | 34.37 |
| B | 0.0574 | 0.0367 | 56.40 |
| C | 0.0511 | 0.0384 | 33.07 |
| D | 0.0565 | 0.0370 | 52.70 |

2.2.1.2 Inter-Hole Distances

Inter-hole distances were also measured, and means and standard deviations calculated (Table 2).

Table 2. Inter-Hole Distances

| Holes | Mean Distance (mm) | Standard Deviation |
|--------------|---------------------------|---------------------------|
| AB | 0.52 | 1.62E-02 |
| BC | 0.41 | 8.17E-03 |
| CD | 0.49 | 1.55E-02 |
| DA | 0.50 | 1.44E-02 |

2.2.1.3 Distortion

For example, Hole A in Slice #0630 (Figure 6) exhibited a non-circular distorted shape of:

Diameter (major length at 151.9 degree) = 0.28 mm.

Diameter (minor length at 64.0 degree) = 0.24 mm.

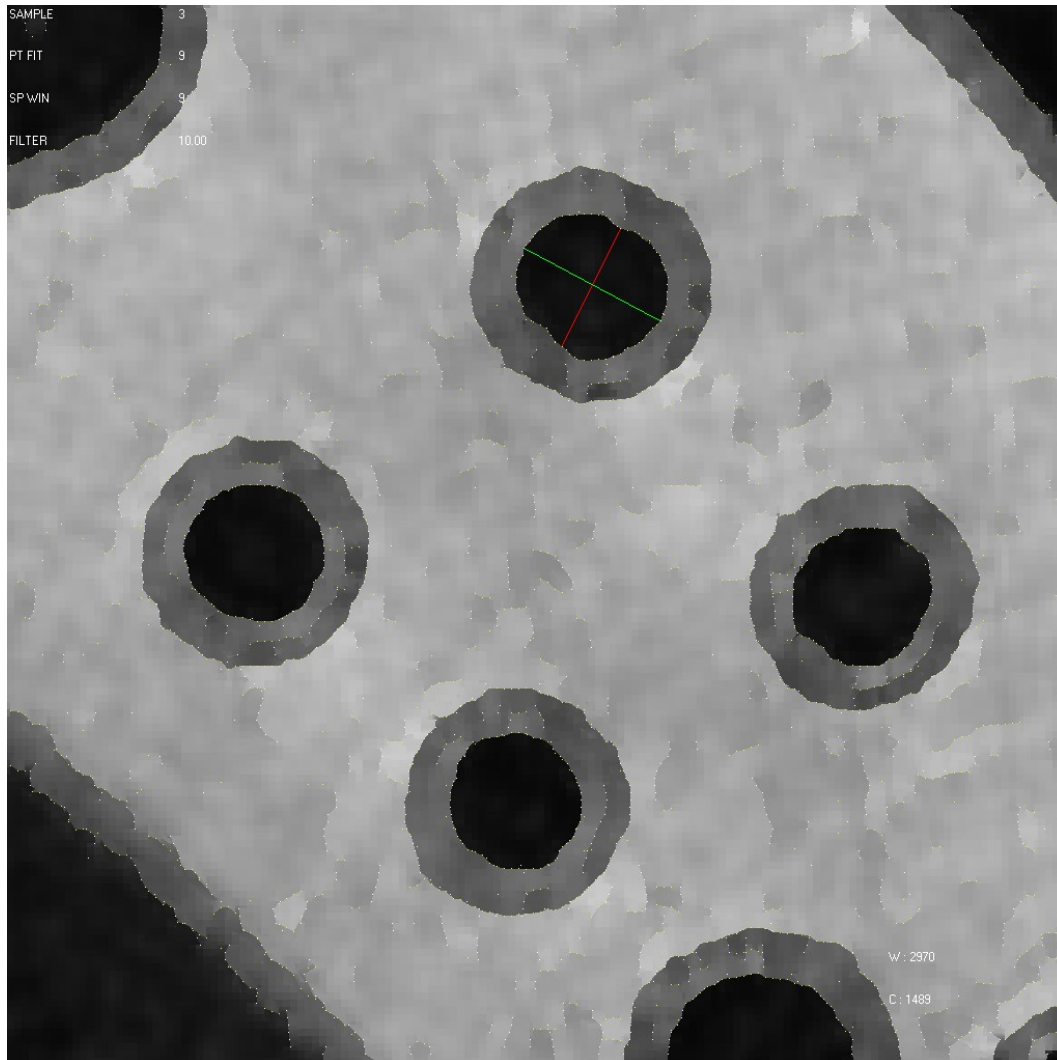


Figure 6. Distortion at Hole A of Slice #0630

2.2.1.4 Fractures

Small fractures were observed at Hole D in Slice #0850 (Figure 7) and at Hole B in Slice #0885 (Figure 8).

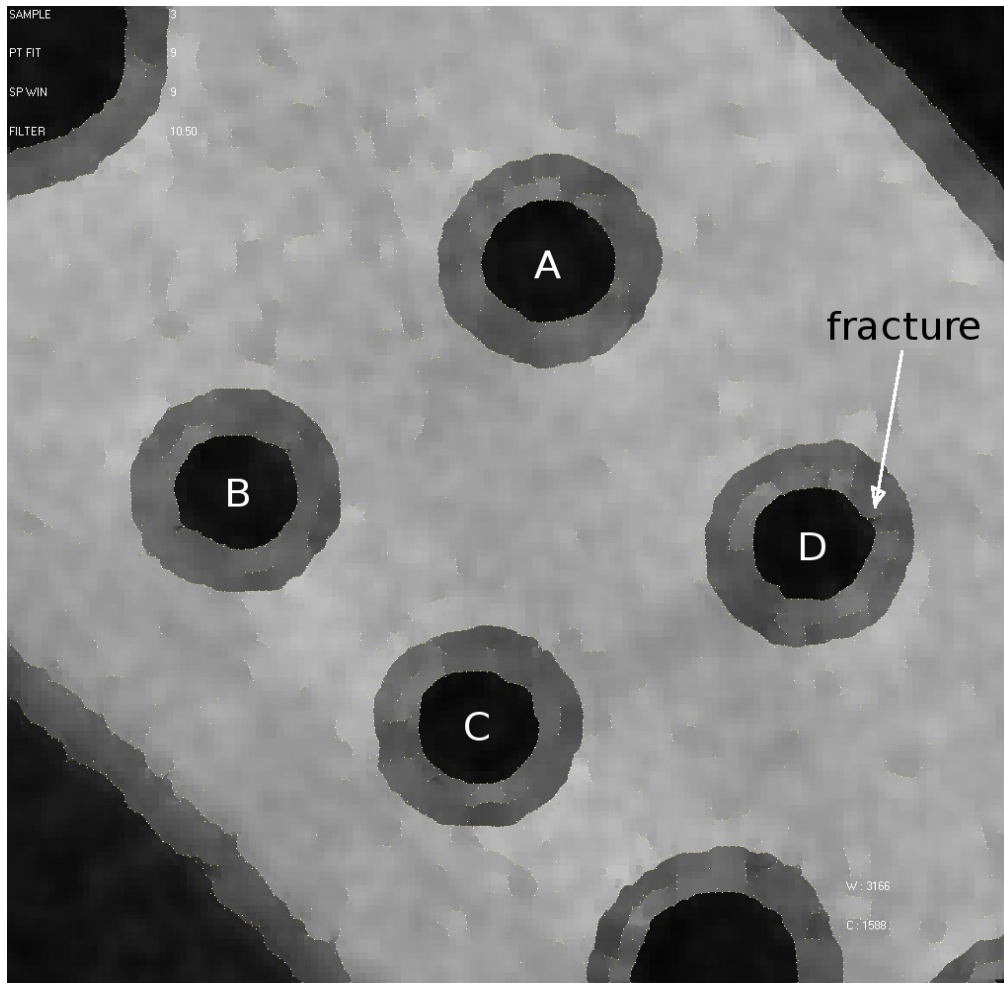


Figure 7: Fracture at Hole D of Slice #0850

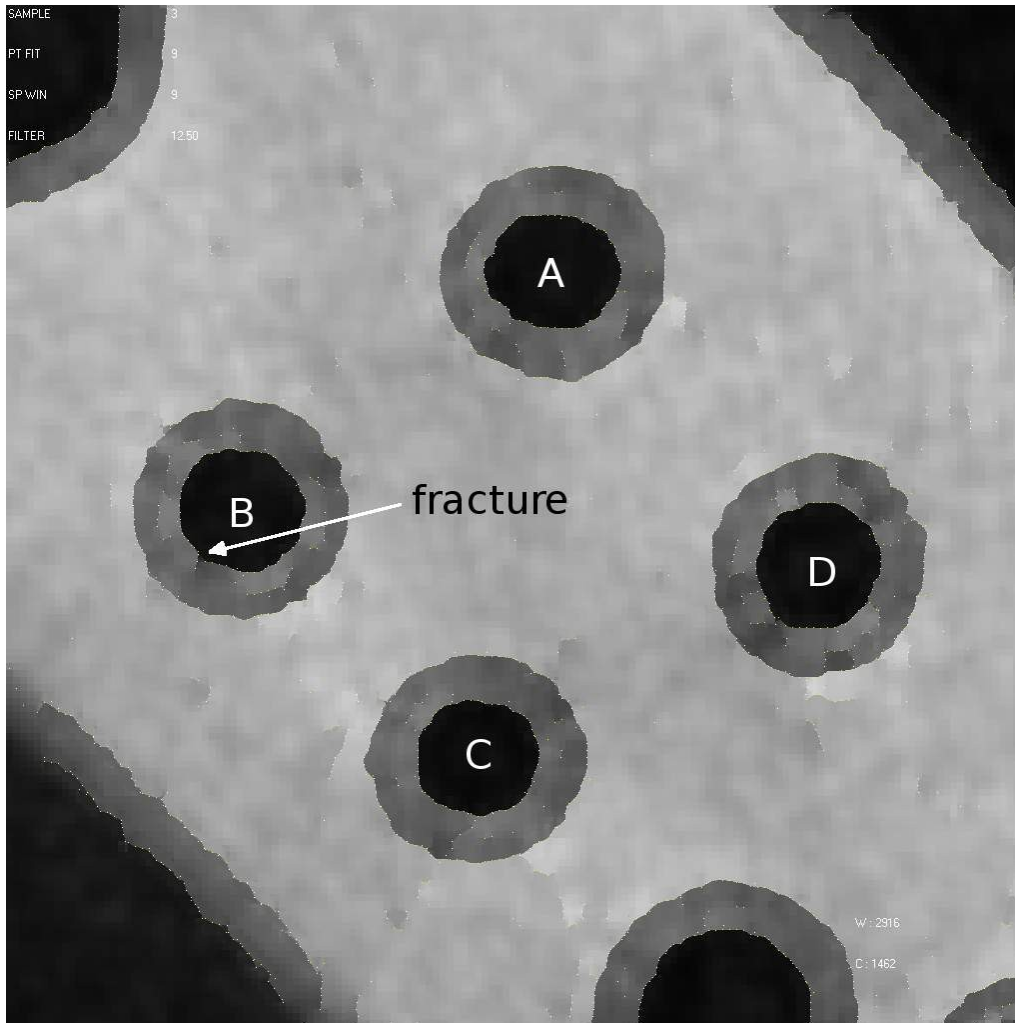


Figure 8: Fracture at Hole B of Slice #0885

3. Conclusions

Detection of minute defects and hyper-accurate area and width measurements of small structures are now possible. The technique may be used for:

- (a) Quality control during the original manufacturing process of components.
- (b) The monitoring of the condition of in-service components prior to reuse.

References

1. "A De-Convolution Technique used for NDT in X-ray & CT", by Kui M. Chui, Shyr L. Chui, Andrew Wride, & David B. Stanfield, Oral/Full paper presentation in 17th World Conference on Non-destructive Testing (17WCNDT), Shanghai, China, October 25-28, 2008. (www.NDT.net - The e-Journal & Database of Non-Destructive Testing - ISSN 1435-4934).
2. "The ICON beamline - A facility for cold neutron imaging at SINQ", by A. Kaestner, S. Hartmann, G. Kuehne, G. Frei, C. Gruenzweig, L. Josic, F. Schmid, E. Lehmann, Nuclear Instruments and Methods in Physics Research Section A: Accelerators, Spectrometers, Detectors and Associated Equipment 659(1), 2011, pp. 387-393.
3. "The line spread function and modulation transfer function of a computed tomographic scanner". Judy P.F., Med. Phys. Vol.3, No. 4, Jul/Aug. 1976, pp.233-236.